

# Influence of Maleic Anhydride on the Compatibility of Thermal Plasticized Starch and Linear Low-Density Polyethylene

Shujun Wang, Jiugao Yu, Jinglin Yu

School of Science, Tianjin University, Tianjin 300072, China

Received 25 August 2003; accepted 1 December 2003

DOI 10.1002/app.20416

Published online in Wiley InterScience (www.interscience.wiley.com).

**ABSTRACT:** In the presence of dicumyl peroxide, the compatibility of thermal plasticized starch/linear low-density polyethylene (TPS/LLDPE) blends using maleic anhydride (MAH) as compatibilizer was investigated. The thermal plasticization of starch and its compatibilizing modification with LLDPE was accomplished in a single-screw extruder at the same time. We prepared three types of blends containing different percentages of TPS and MAH. The content of MAH based on LLDPE was 0, 1, and 2 wt %, respectively. The morphology of the blends was studied by SEM. It was found that, with the addition of MAH, the blends have good interfacial adhesion and finely dispersed TPS and LLDPE phases, which is reflected in the mechanical

and thermal properties of the blends. The blends containing MAH showed higher tensile strength, elongation at break, and thermal stability than those of blends without MAH. The rheologic properties of the blends demonstrated the existence of processing. Finally, the dynamic thermal mechanical analysis results indicated that, with the addition of MAH, the compatibility between TPS and LLDPE in the blends was substantially improved. © 2004 Wiley Periodicals, Inc. *J Appl Polym Sci* 93: 686–695, 2004

**Key words:** starch; polyethylene (PE); blends; compatibility; rheology

## INTRODUCTION

Over the last 50 years, synthetic polymers have become the major new materials replacing the traditional ones such as paper, glass, steel, and aluminum in many applications.<sup>1</sup> These new synthetic polymers have many advantages, such as high tensile strength and elongation at break, and are easily produced into various end products with desirable properties. The polymers also have some disadvantages, however, mainly the nonbiodegradability that causes many environmental problems. Various approaches to render synthetic polymers degradable have been considered. The earliest method was the addition of native starch granules to low-density polyethylene (LDPE), which was found in Griffin's patents.<sup>2–4</sup> However, these materials had poor tensile strength, elongation at break, and biodegradability. As a result of these efforts, several commercial products have been developed over the last few years, but most of them contain relatively low amounts of starch because increasing the amount of starch would induce a decrease in both tensile strength and elongation at break.<sup>5</sup> This deterioration arises from the different polar characteristics of starch

and most of the synthetic polymers, which lead to poor interfacial adhesion. To increase the interfacial adhesion and further improve the mechanical properties, a compatibilizer must be used.

The ethylene–acrylic acid (EAA) copolymer is the most effective compatibilizer used so far, but it must be used in large amounts to achieve satisfactory mechanical properties. Otey et al.<sup>6,7</sup> produced blown films containing up to 40–50 wt % gelatinized starch along with EAA and ammonia. The carboxylic groups of EAA can form V-type complexes with the hydroxyl groups of starch,<sup>8,9</sup> increasing the tolerated amounts of starch in the blends, in which case it could lower the biodegradation rate of starch.<sup>10</sup> On the other hand, EAA has an accelerating effort on thermooxidative degradation of LDPE/starch blends when used in low amounts, together with a prooxidant.<sup>11</sup>

Complexes similar to EAA can also be formed with hydroxyl groups of the polyethylene–vinyl alcohol (EVOH) copolymer.<sup>12</sup> As a result, materials with high amounts of starch can be produced. Also, the addition of EVOH can increase the processing ability and injection moldability of plasticized starch.<sup>13</sup> Poly(vinyl alcohol), however, is water soluble, thus limiting the use of such materials in aquatic environments.

In the last few years, increased interest has developed with respect to starch together with polymers containing reactive groups, such as copolymers of styrene–maleic anhydride (SMA), ethylene–propylene–

Correspondence to: J. Yu (edwinwa@hotmail.com).

maleic anhydride (EPMA), propylene-glycidyl methacrylate (PGMA), and ethylene-maleic anhydride (EMA),<sup>14-17</sup> although these copolymers are expensive and difficult to produce. In the present study, we first used MAH as the compatibilizer in a thermal plasticized starch/linear low-density polyethylene (TPS/LLDPE) system, in the presence of dicumyl peroxide. The main objective was to test the compatibility of these blends.

## EXPERIMENTAL

### Materials

The linear low-density polyethylene (LLDPE 7042) was purchased from Jilin Petrochemical Filiale (Jilin, China). The native corn starch (ST, 11% moisture), containing 30 wt % amylose and 70 wt % amylopectin, was obtained from Langfang Starch Co. (Langfang, Hebei, China). The plasticizer, glycerol, was purchased from Tianjin Chemical Reagent Factory (Tianjin, China). Maleic anhydride (MAH), purchased from Tianjin Chemical Reagent Factory, was recrystallized twice with  $\text{CHCl}_3$  before use. Dicumyl peroxide (DCP), obtained from Shanghai Chemical Reagent Co., China Pharmacy Group (Shanghai, China), was recrystallized with absolute alcohol before use.

### Sample preparation

Blending was carried out by use of a high-speed mixer GH-100Y (made in China) at room temperature. The rotor rate was maintained at 3000 rpm for 2 min, adding LLDPE and starch first, then adding glycerol, MAH, and DCP. The mixtures were manually fed into a laboratory-scale single-screw extruder [SJ-25(S), screw diameter ( $d$ ) = 30 mm; length-to-diameter (L/D) ratio = 25 : 1; made in China]. The extrusion conditions were as follows: the temperature profile along the extruder barrel: 140–145–150–130°C (from feed zone to die); the screw speed was 15 rpm. The die was a round sheet with 3-mm-diameter holes. For TPS/LLDPE blends, five different levels of TPS were used: 50, 60, 70, 80, and 90 wt %. MAH and DCP were used as monomer and initiator at 1 and 0.1 wt % levels based on LLDPE, respectively. Some extrudates were hot pressed into thin films at 110–120°C and 10 kN for 15 min, for dynamic mechanical analysis. The level of glycerol in the blends was 30 wt % based on the native corn starch. The detailed compositions of samples are listed in Table I.

### Scanning electron microscopy (SEM)

Specimens were fractured after being frozen in liquid nitrogen and the exposed surfaces were observed with an environmental electron microscope (ESEM, Philips

TABLE I  
Samples Codes and Composition of Raw Materials

Sample code	Raw materials				
	LLDPE	ST	GL	MAH	DCP
1	50	38.5	11.5	—	—
2	40	46.2	13.8	—	—
3	30	53.8	16.2	—	—
4	20	61.5	18.5	—	—
5	10	69.2	20.8	—	—
6	50	38.08	11.37	0.5	0.05
7	40	45.81	13.75	0.4	0.04
8	30	53.59	16.08	0.3	0.03
9	20	61.37	18.41	0.2	0.02
10	10	69.15	20.74	0.1	0.01
11	50	37.65	11.30	1.0	0.05
12	40	45.51	13.65	0.8	0.04
13	30	53.36	16.01	0.6	0.03
14	20	61.22	18.36	0.4	0.02
15	10	69.07	20.72	0.2	0.01

XL-3, The Netherlands). All surfaces were coated with gold to avoid charging under the electron beam. The electron gun voltage was set at 30 kV. The micrographs of samples were taken at magnifications of  $\times 500$  to identify cracks, holes, and other changes on the surface of the samples in either the presence or the absence of MAH.

### Mechanical properties of blends

Measurements of the mechanical properties, such as tensile strength and elongation at break, were performed according to the method detailed in ASTM D828-88 (ASTM 1989) on a WD-5 electron tester. Measurements were done using a 100 mm/min crosshead speed. Before the measurement, the samples were conditioned at  $50 \pm 5\%$  relative humidity for 48 h at an ambient temperature in a closed chamber containing a 33.46 wt %  $\text{CaCl}_2$  solution in a beaker. Ten measurements were conducted for each sample and the results were averaged to obtain a mean value. The measurements are reported as the relative mechanical property (i.e., ratio of a mechanical property of the blend to that of neat LLDPE) in all cases.

### Thermogravimetric analysis (TGA)

The thermal properties of the blends were measured with a ZTY-ZP type thermal analyzer. The sample weight varied from 10 to 15 mg. Samples were heated from ambient temperature to 500°C at a heating rate of 15°C/min. Derivatives of TGA thermograms were obtained using Origin 6.0 analysis software (RockWare Inc., Golden, CO).

### Rheology

The extruded strips were cut into small pieces, which were tested by an XYL-II capillary rheometer. The

capillary radius was 1 mm and  $L/D$  was 40. The small pieces were placed into the barrel through a funnel and then packed down with the plunger until the first extrudate appeared at the capillary exit. The samples were allowed to come to temperature (balancing for 10–15 min), and were then forced through the capillary by the plunger at preselected velocities. The next velocity in the measure schedule began when the load versus extension curves reached a slope close to zero. The load on the plunger and plunger speed provided the total pressure drop through the barrel and capillary and the volume flow rate. Shear rate ( $\dot{\gamma}$ ) and shear stress ( $\tau$ ) were calculated by standard methods. To understand the processing properties of TPS/LLDPE blends, the rheology experiments were conducted at 125°C, which covered the processing temperature range.

### Dynamic mechanical thermal analysis (DTMA)

DTMA, using a Mark Netzsch DMA242 analyzer (Netzsch-Gerätebau GmbH, Bavaria, Germany), was used on hot-pressed thick specimens ( $\sim 2.0 \times 11 \times 16$  mm), in a single-cantilever bending mode at a frequency of 3.33 Hz and a strain  $\times 2$  N, corresponding to a maximum displacement amplitude of 30  $\mu\text{m}$ . The analyzer compared the stress and strain signals and resolved the strain into the in-phase (storage) and out-of-phase (loss) components, from which storage or elastic ( $E'$ ) and loss ( $E''$ ) moduli, as well as the  $\tan \delta$  ( $= E''/E'$ ), were obtained as a function of temperature. The range of temperature was from  $-100$  to  $100^\circ\text{C}$ , at a standard heating rate of  $3.0^\circ\text{C}/\text{min}$ . Samples were coated with silicone wax to prevent water from evaporating during heating. For polymeric materials a decrease in storage modulus and a peak in  $\tan \delta$  are used as indicators of glass transition.

## RESULTS AND DISCUSSION

### Blend morphology

In polymer blends, it is necessary to study the morphology of the final product because most of its properties, especially its mechanical properties, depend on it. In most cases, the major components of the blends form the continuous phase, whereas the minor components constitute the dispersed phase. However, as the volume fraction of the minor components increases to a certain volume, the process will transfer from the dispersed phase to the continuous phase.<sup>18</sup> Thus, in our present study, for a blend with high starch content, starch is expected to be the continuous phase and LLDPE is the dispersed phase.

Another parameter affecting the morphology and properties of polymeric blends is the use of compatibilizer. Preliminary studies showed that a finer and

more uniform dispersion of starch in the LDPE matrix could be achieved in the blends compatibilized with PE-*g*-MAH copolymers.<sup>19</sup> To see the interfacial structure between the matrix and the dispersed phase, SEM micrographs of fracture surfaces were obtained and are shown in Figure 1.

Figure 1(a), (b), and (b') are SEM micrographs of samples 1, 6, and 11, respectively. As can be seen from Figure 1(a), many starch particles were obviously not disrupted and some of them were removed from the surface of the sample during the fracture of the specimen, leaving some cavities in the fracture surface, presumably because of the weak interfacial adhesion between TPS and LLDPE. Because most of the starch particles still remained on the fracture surface, the starch phase appeared to be practically separated from the LLDPE. Besides, the average size of starch particles was about 10  $\mu\text{m}$ , whereas the native corn starch particle was about 15  $\mu\text{m}$  in diameter. In Figure 1(b) and (b'), we can scarcely see the separated starch particles, and there was no apparent phase interface between TPS and LLDPE; the average size of the starch particles was about 5  $\mu\text{m}$ . Moreover, the fracture surface did not have cavities because the starch particles were not removed from the fracture surface during the preparation of SEM samples. These facts indicated that the interfacial adhesion of the blends with addition of MAH is improved.

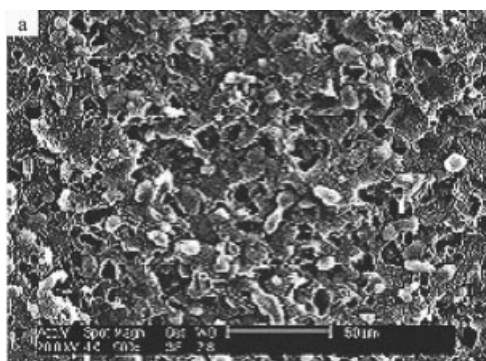
Blends containing up to 60, 70, 80, and 90 wt % TPS exhibited the same phenomenon, that is to say, the blends with the addition of MAH have better microscopic morphology than that of blends without the addition of MAH.

### Mechanical properties

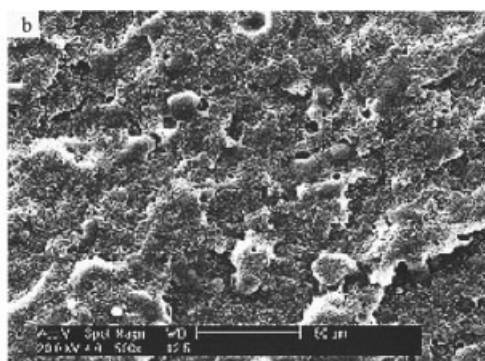
Figures 2 and 3 show the effect of TPS content on the relative tensile strength and relative elongation at break of samples, respectively. The variation in the relative tensile strength and relative elongation at break of samples with MAH content is also shown in the figures.

As observed from Figures 2 and 3, the relative tensile strength and the relative elongation at break were decreased with increasing TPS content for all samples, regardless of the existence of MAH. This general phenomenon was because of the presence of starch particles, which do not contribute to the mechanical properties of the blends, and has been observed in many studies.<sup>20–22</sup> However, the main purpose was to test the effect of MAH on the mechanical properties of TPS/LLDPE blends.

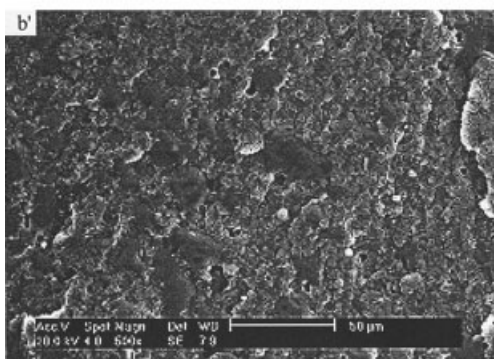
As is well known, the starch granule is highly hydrophilic, containing hydroxyl groups on its surface, whereas LLDPE is basically nonpolar. Therefore, the formation of the strong interfacial bonds such as hydrogen bonds is not feasible. As a result, when stress



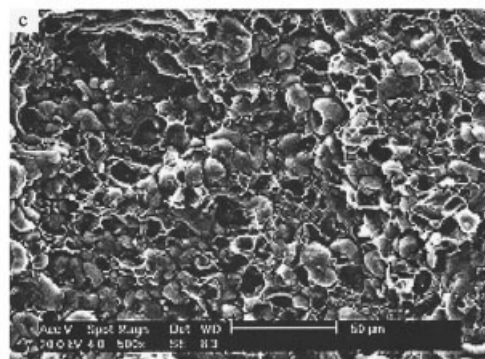
a) SEM photograph of sample 1



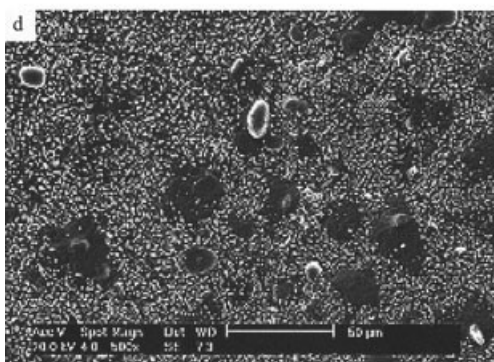
b) SEM photograph of sample 6



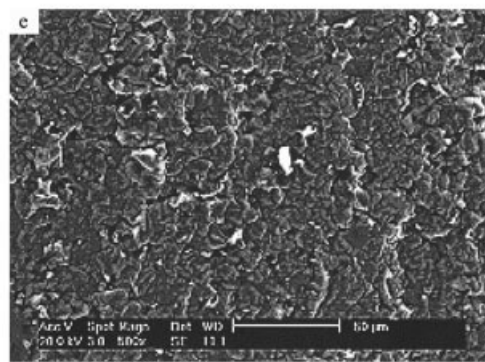
b') SEM photograph of sample 11



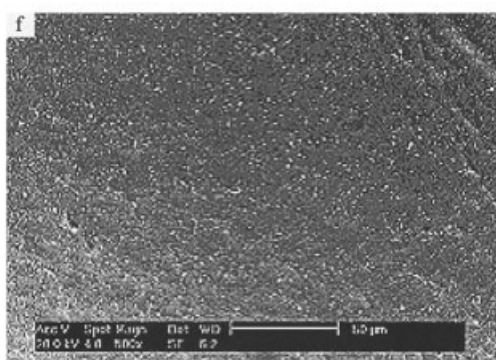
c) SEM photograph of sample 3



d) SEM photograph of sample 8



e) SEM photograph of sample 5



f) SEM photograph of sample 10

**Figure 1** SEM micrographs of the surface of samples: (a) sample 1; (b) sample 6; (b') sample 11; (c) sample 3; (d) sample 8; (e) sample 5; (f) sample 10.

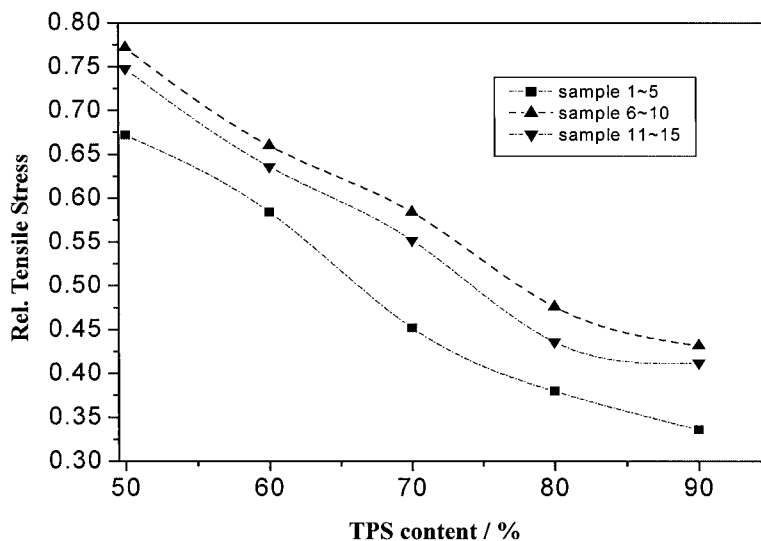


Figure 2 Relative tensile stress of samples.

was exerted on the blends, the fracture resistance of the blends without the addition of MAH was not improved. However, the relative tensile strength and the relative elongation at break of the samples were improved with the addition of MAH. The addition of MAH substantially strengthened TPS and LLDPE interfacial adhesion; this increased interfacial adhesion for the blends was believed to be attributed to the chemical reaction of MAH groups with hydroxyl groups on starch at the interface. However, further increases in the MAH content reduced the relative tensile strength and the relative elongation at break. Nonetheless, on the other hand, the compatibility was improved with increasing MAH content. The increasing content of MAH would critically suppress TPS and LLDPE, and the mechanical properties of the final product would be impaired.

Factorial analysis of the experimental data was performed and nonlinear regression equations for the relative tensile strength (RTS) and the relative elongation at break (REB) were obtained, as follows:

$$\begin{aligned} \text{RTS} = & 1.61719 - 0.02497(\text{TPS}) + 0.53002(\text{C}) \\ & + 0.00012(\text{TPS})^2 - 0.35066(\text{C})^2 - 0.00269(\text{TPS})(\text{C}) \end{aligned} \quad r = 0.99 \quad (1)$$

$$\begin{aligned} \text{REB} = & 0.59695 - 0.01548(\text{TPS}) + 0.74235(\text{C}) \\ & + 0.00011(\text{TPS})^2 - 0.18747(\text{C})^2 - 0.00829(\text{TPS})(\text{C}) \end{aligned} \quad r = 0.92 \quad (2)$$

In the two equations, TPS and C refer to the contents of TPS and MAH in the blends, respectively.

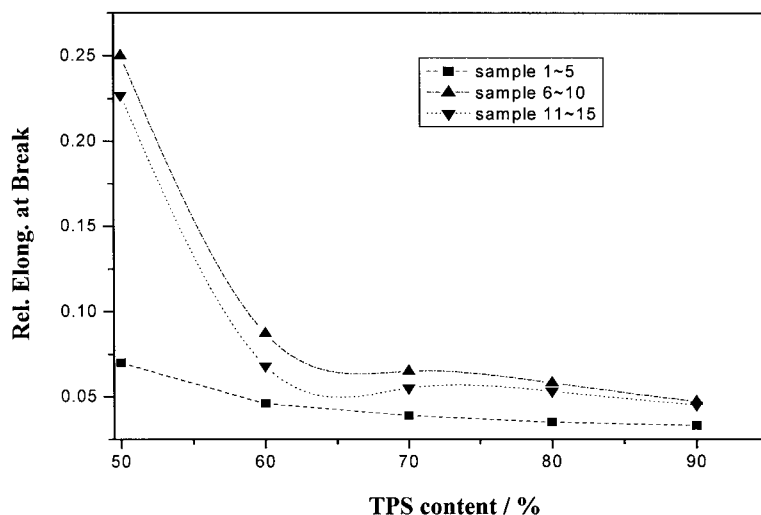


Figure 3 Relative elongation at break of samples.

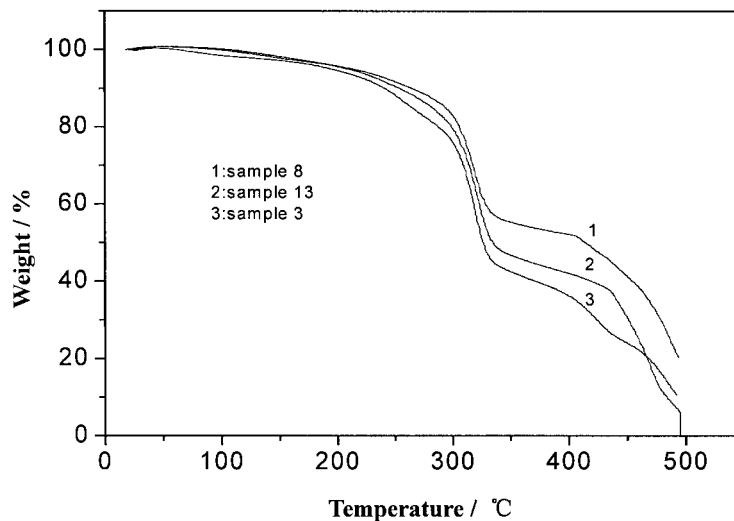


Figure 4 TG thermogram of samples.

As can be seen from Figures 2 and 3, the improvement in the mechanical properties of blends was not significant for two reasons: (1) in the blends without the addition of MAH, the rigid starch particles were slightly disrupted, although with the addition of MAH, the rigid starch particles were destroyed completely, and the rigid starch particles could resist higher stress than the plasticized starch particles; (2) it was not clear at this moment how the MAH groups were exactly distributed in the blends. Even though some of the MAH groups appeared to be situated at the interface between TPS and LLDPE phases, thus enhancing the interfacial adhesion, some might be included in the LLDPE phase. If some fractions of MAH groups formed micellar domains in the LLDPE phase, those would not contribute to the improvement of the interfacial adhesion strength. Furthermore, such

a micellar structure might diminish the mechanical properties of the blends.

#### TGA

Figures 4 and 5 show TG thermograms of samples 3, 8, and 13, and samples 6, 7, 8, 9, 10, respectively.

As obtained from Figures 4 and 5, three well-defined shifts were observed in the TG curves. The first shift, at around 100°C, was produced by water evaporation or the unreacted MAH sublimation; the second shift started at 180°C and was attributed to the evaporation of glycerol. This process continued gradually up to 300°C, where the thermal degradation of starch occurred; the last shift, at around 400°C, was caused by the thermal decomposition of LLDPE.

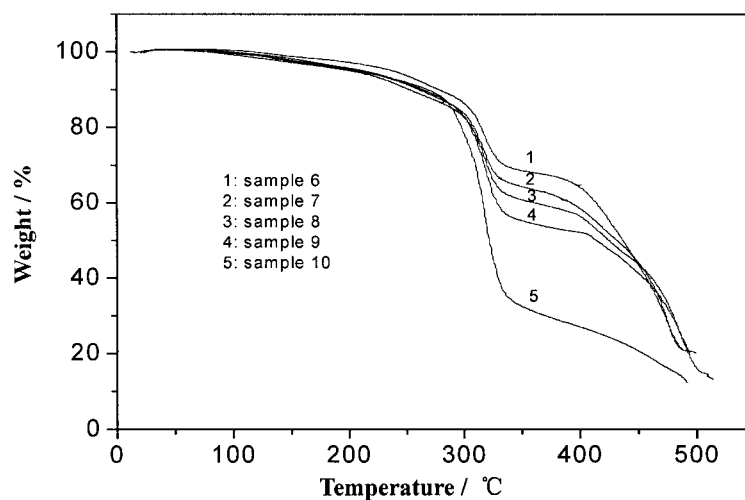


Figure 5 TG thermogram of samples.

TABLE II  
TG Percentage of Samples

Sample	TPS content (%) 25°C	Weight loss (%) 400°C	Error (%)
1	50	49.2	2
11	49.45	39.7	21.1
6	48.95	32.5	34.6
2	60	58.4	3.33
12	59.56	49.3	17.7
7	59.15	40.2	32.4
4	80	78.1	2.5
14	79.78	68.5	14.8
9	79.58	49.4	38.4
5	90	91.7	1.11
15	89.89	81.6	9.89
10	89.79	72.8	19.81

At around 400°C, the total weight loss of sample 3 was 68 wt %. The data were in agreement with the TPS content. However, the data were 58 and 48 wt %, corresponding to samples 13 and 8, respectively. Before 400°C, the weight loss of samples was mainly caused by the thermal degradation of TPS. According to the content of TPS of samples, the reduction in weight loss was the result of the improvement in the thermal stability. The other samples, with equal loading of TPS, followed a similar trend. Table II shows the weight loss of other samples at 400°C. The improvement in thermal stability also confirmed that, with the addition of MAH, the adhesion between TPS and LLDPE in the blends was enhanced, further improving the compatibility of TPS and LLDPE. However, with increasing MAH content, the thermal stability of samples decreased, perhaps attributable to the deterioration of DCP and MAH on TPS and LLDPE during extrusion. From Figure 5, we can see that with increas-

ing LLDPE content, the thermal stability of samples was enhanced.

### Rheology

The data for the shear stress and the apparent viscosity as a function of shear rate are shown in Figures 6 and 7, respectively.

As observed from Figures 6 and 7, with increasing shear rate, the apparent viscosity of the three samples evidenced a declining trend, and such flow behavior was designated shear thinning. The samples exhibited power-law behavior, which was ascribed to the gradual deterioration of intermolecular action between starch and LLDPE. The apparent viscosity of samples 6 and 11 was lower than that of sample 1 at the same shear rate, which was closely related to the molecular realignment. In sample 1, TPS and LLDPE were not well dispersed (shown in SEM micrographs), and the adhesion between TPS and LLDPE was poor. The rigid starch particles and the molecular orientation prevented the blend melt from flowing smoothly at the experimental temperature, so apparent viscosity is high. In samples 6 and 11, however, the arrangement of molecules was more orderly than that of sample 1 because of the good plasticization of starch and good compatibility between TPS and LLDPE. So the action of rigid starch particles and the molecular orientation were decreased under the shear stress. Consequently, the blend melt reduced the flow friction obstruction and produced the lower apparent viscosity. The viscosity of sample 6 was higher than that of sample 11 as a result of the substantial destruction of MAH acting on the TPS and LLDPE.

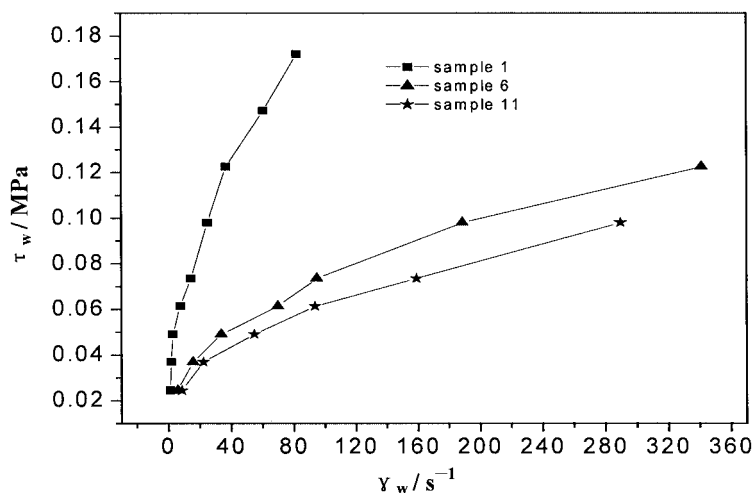


Figure 6  $\tau_w \sim \gamma_w$  curves of samples at 125°C.

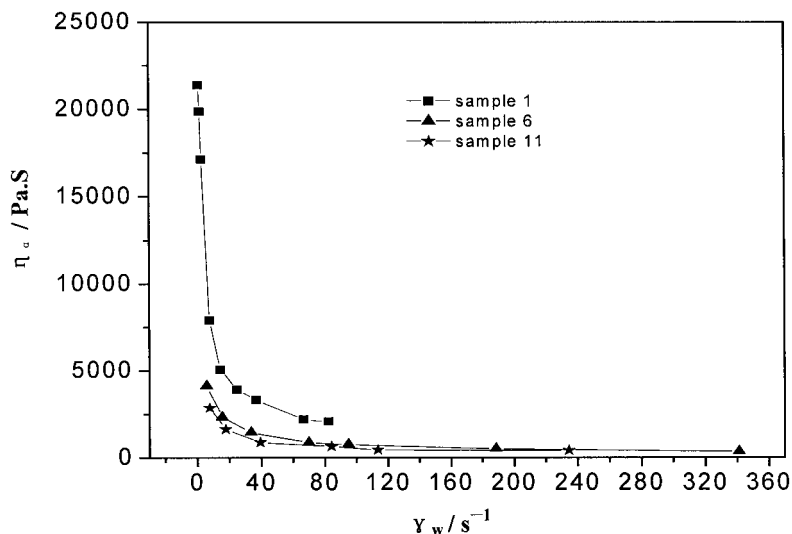


Figure 7  $\eta_a \sim \gamma_w$  curves of samples at 125°C.

#### DTMA

The dynamic thermal mechanical data for the blends, that is, the storage moduli ( $E'$ ) and the loss factor ( $\tan \delta$ ) as a function of temperature, are shown in Figures 8 and 9, respectively.

Storage modulus is an important parameter of the rigidity of materials. As can be seen from Figure 8, the storage moduli of samples 6 and 8 were lower than those of samples 1 and 3, which was related to the plasticization of starch. The plasticization of starch in samples 6 and 8 was better than that in samples 1 and 3 (which can be seen in SEM micrographs). Some particles, called agglomerates, were always in contact with each other. Rigid agglomerates of samples 1 and 3, in which there was no motion at particle-particle contact points, increased the modulus more than that found in samples 6 and 8, in which TPS and LLDPE

were perfectly dispersed and there were only a few rigid starch particles.

As reported in the literature,<sup>23,24</sup> the glass-transition temperature ( $T_g$ ) of LLDPE is around  $-80$  to  $-120^\circ\text{C}$ ; that of the plasticized starch with glycerol is  $40$ – $60^\circ\text{C}$ . As can be seen from Figure 9, the four samples all exhibited two glass-transition temperatures, all between that of pure TPS and that of LLDPE, corresponding to LLDPE ( $<0^\circ\text{C}$ ) and TPS ( $>0^\circ\text{C}$ ). Thus TPS and LLDPE in the samples were not compatibilized at the molecular level. However, by comparing the blends with MAH and those without MAH, we found that the glass-transition temperatures of TPS and LLDPE in samples 6 and 8 were closer than they were in samples 1 and 3. Although the compatibility at the molecular level was impossible, the interaction power between TPS and LLDPE in the sample was improved

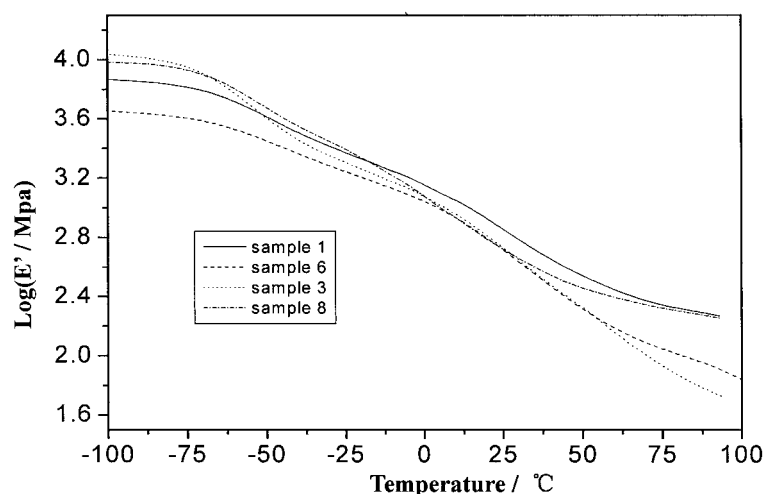


Figure 8 DMA thermogram of samples: storage modulus.



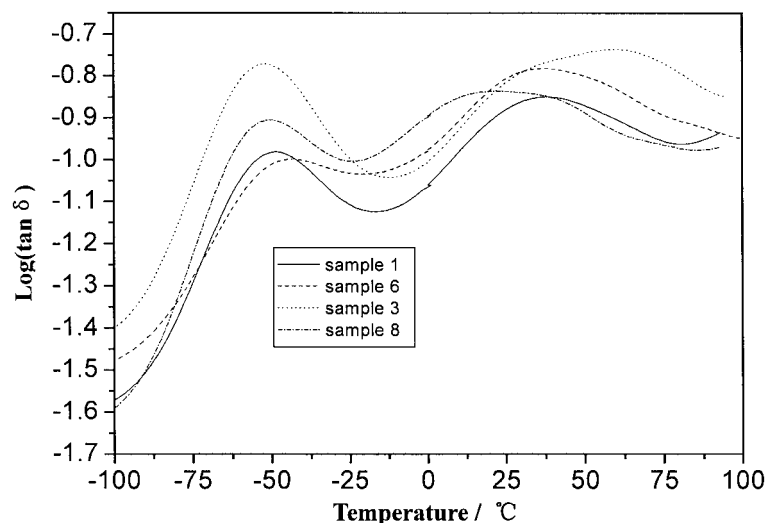


Figure 9 DMA thermogram of samples:  $\tan \delta$ .

with the addition of MAH, thus increasing the compatibility of TPS and LLDPE. We did not obtain a continuously uniform system, although the improvement in compatibility promoted good mechanical properties and thermal stability in the blends.

### Mechanism of compatibility

Reasons for incompatibility of TPS/LLDPE blends are high interfacial tension and, consequently, poor interfacial adhesion between the two components. However, the phenomenon of compatibility can be induced in an immiscible binary system by introducing a third component that either will interact chemically with both phases or will have specific interaction with one phase and physical interaction with the other. The addition of a block or graft copolymer reduces the interfacial tension between the two phases, increases the surface area of the dispersed phase, promotes adhesion between the phase components, and stabilizes the dispersed phase morphology.<sup>25</sup>

Investigation of PE-g-MAH, used as compatibilizer between starch and PE, was reported in a number of studies in the literature.<sup>18,26–28</sup> A uniform viewpoint that PE-g-MAH was used as compatibilizer is based on two factors: (1) the ester-forming ability of anhydride groups with hydroxyl groups on starch, the hydrogen bond-forming ability between carboxyl groups of hydrolyzed MAH and hydroxyl groups on starch; (2) the substantial compatibility between grafted PE chain and PE phase. The mechanism is illustrated as follows.

On the basis of this concept, we designed an experiment that, at the same extruded conditions, LLDPE and MAH were simultaneously extruded in the presence of DCP, and the extrudate was purified to remove the unreacted MAH and small molecules. The purified method was as follows: dissolution of modified LLDPE in xylene followed by precipitation in acetone.<sup>29</sup> FTIR spectra of the grafted product and pure LLDPE are shown in Figure 11. By comparing the pure LLDPE with the grafted product, we observed

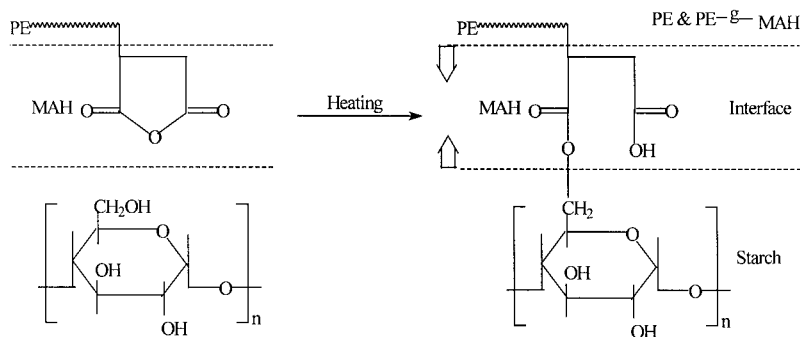
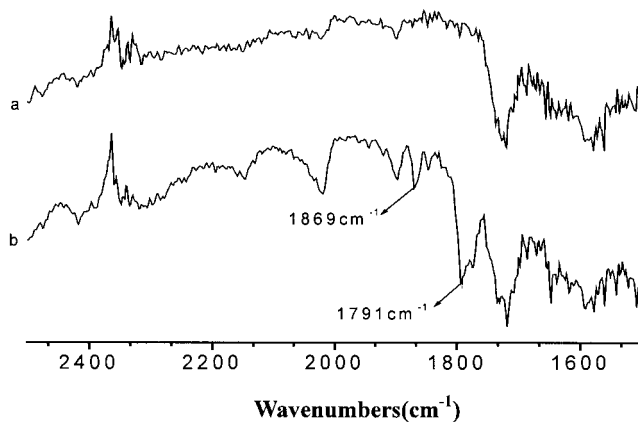


Figure 10 Interfacial chemical reaction of MAH and OH.



**Figure 11** FTIR spectra of PE and PE-g-MAH. (a) PE; (b) PE-g-MAH.

the symmetrical and asymmetrical stretching vibration bonds of anhydride groups at 1869 and 1791  $\text{cm}^{-1}$ , respectively. This verified the fact that MAH grafted onto LLDPE in the presence of DCP, and was used as a compatibilizer in the TPS/LLDPE blends during the extrusion.

### CONCLUSIONS

In the presence of DCP, TPS and LLDPE were compatibilized with the addition of MAH. The blends with the addition of MAH have higher tensile strength, elongation at break, and thermal stability than those of the blends without the addition of MAH. With increasing MAH content, the mechanical and thermal properties of the blends decreased, which is probably attributable to the deterioration of MAH to the starch particle and LLDPE in the presence of DCP during the extrusion. Another important finding is that the blends with the addition of MAH have better flow behavior, which arises from two factors: (1) the good arrangement of TPS and LLDPE; (2) the deterioration of MAH to the starch particle and LLDPE, thus causing the molecular weight of TPS and LLDPE to decrease. All of the above phenomena are ascribed to the improvement in the compatibility between TPS and LLDPE.

### References

- Guillet, J. In: *Degradable Polymers: Principles and Applications*, 1st ed.; Scott, G.; Gilead, D., Eds.; Chapman & Hall: London, 1995; pp. 216–246.
- Griffin, G. J. L. U.S. Pat. 4,016,177, 1977.
- Griffin, G. J. L. U.S. Pat. 4,021,388, 1977.
- Griffin, G. J. L. U.S. Pat. 4,125,495, 1978.
- Evangelista, R. L.; Nikolov, Z. L.; Sung, W.; Jane, J. L.; Gelina, R. L. *Ind Eng Chem Res* 1991, 30, 1841.
- Otey, F. H.; Westhoff, R. P.; Doane, W. M. *Ind Eng Chem Prod Res Dev* 1980, 19, 592.
- Otey, F. H.; Westhoff, R. P.; Doane, W. M. *Ind Eng Chem Prod Res* 1987, 26, 1659.
- Fanta, G. F.; Swanson, C. L.; Doane, W. M. *J Appl Polym Sci* 1990, 40, 811.
- Shogren, R. L.; Green, R. V.; Wu, Y. V. *J Appl Polym Sci* 1991, 42, 1701.
- Imam, S. H.; Gould, S. M.; Kinney, M. P.; Ramsay, A. M.; Tosyeson, T. R. *Curr Microbiol* 1992, 25, 1.
- Bikiaris, D.; Prinos, J.; Panagiotou, C. *Polym Degrad Stab* 1997, 56, 1.
- Bikiaris, D. In: *Degradable Polymers: Principles and Applications*, 1st ed.; Scott, G.; Gilead, D., Eds.; Chapman & Hall: London, 1995; p. 112.
- George, E. R.; Sullivan, T. M.; Park, E. H. *Polym Eng Sci* 1994, 34, 17.
- Nie, L.; Narayan, R.; Grulke, E. A. *Polymer* 1995, 36, 2227.
- Yang, Z.; Bhattacharya, M.; Vaidya, U. R. *Polymer* 1996, 37, 2137.
- Vaidya, U. R.; Bhattacharya, M. *J Appl Polym Sci* 1994, 52, 617.
- Matzions, P.; Bikiaris, D.; Kokkou, S.; Panagiotou, C. *J Appl Polym Sci* 2001, 79, 2584.
- Willemse, R. L.; Posthuma de Boer, A.; van Damand, J.; Gotsis, A. D. *Polymer* 1998, 39, 5879.
- Bikiaris, D.; Panagiotou, C. *J Appl Polym Sci* 1998, 70, 1503.
- Willett, J. L. *J Appl Polym Sci* 1994, 54, 1685.
- Nikolov, Z. L.; Evangelista, R. L.; Wung, W.; Jane, J. L.; Gelina, R. J. *Ind Eng Chem Res* 1991, 30, 1841.
- Kang, B. G.; Yung, S. H.; Jie, J. E.; Yoon, B. S.; Soo, M. H. *J Appl Polym Sci* 1996, 60, 1977.
- Liang, Z.; Williams, H. L. *J Appl Polym Sci* 1992, 44, 699.
- Martin, O.; Averous, L. *Polymer* 2001, 42, 6209.
- Tedisco, A.; Barbosa, R. V.; Nachtigall, S. M. B.; Mauler, R. S. *Polym Test* 2002, 21, 11.
- Seong, I. Y.; Tae, Y. L.; Jin-san, Y.; Ik-mo, L.; Mal-nam, K.; Han, S. L. *J Appl Polym Sci* 2002, 83, 767.
- Bikiaris, D.; Prinos, J.; Koutsopoulos, K.; Vouroutzis, N.; Pavlidou, E.; Frangis, N.; Panagiotou, C. *Polym Degrad Stab* 1998, 59, 287.
- Chandra, R.; Rustgi, R. *Polym Degrad Stab* 1997, 56, 185.
- Bettini, S. H. P.; Agnelli, J. A. M. *Polym Test* 2000, 15, 3.